Optical fiber cable assembly characterization for the Mercury Laser Altimeter

Melanie N. Ott[*a], Marcellus Proctor[b], Matthew Dodson[a], Shawn Macmurphy[a], Patricia Friedberg[b]
[a]Sigma Research and Engineering, NASA GSFC, Greenbelt MD 20771
[b]NASA GSFC, Greenbelt MD 20771

ABSTRACT

For the space flight mission MESSENGER, the Mercury Laser Altimeter (MLA) instrument required highly reliable optical fiber assemblies for the beam delivery system. A custom assembly was designed based on commercially available technologies to accommodate the requirements for the mission. Presented here are the results of environmental testing the MLA optical fiber assemblies. These assemblies consisted of W.L.Gore FLEX-LITE™ cable with 200 micron core Polymicro Technologies optical fiber and the Diamond AVIMS connector kits. The assemblies were terminated to the NASA-STD-8739.5 in the Code 562 Advanced Photonics Interconnection Manufacturing Laboratory at NASA Goddard Space Flight Center. The technology validation methods that were used to characterize these assemblies for usage in a space flight environment have been established and well documented.[1-4] Only the tests that are known to bring out the failure modes typical to optical fiber assemblies have been performed to assess the ability of these assemblies to withstand the environmental parameters that have been established for Mercury Laser Altimeter. Testing involved vacuum, vibration, thermal and radiation exposure and the data with results of those characterization tests are included here. For the radiation characterization, both the 200 micron core FLEX-LITE™ (FON1173) and the 300 micron core FLEX-LITE™ (FON1174) were tested. For all other environmental tests only the 200 micron core FLEX-LITE™ /AVIMs assembly was tested since it was expected that the results of such testing would not differ much with core size.
Keywords: optical fiber, assemblies, characterization, spaceflight, Diamond, connector, environmental, radiation.

1. INTRODUCTION

All FLEX-LITE™ with AVIMS assemblies were manufactured in the APIM laboratory of the NASA Code 562 Component Technologies Office. A materials study was performed during the GLAS mission as well as for MLA with some testing performed for materials in which data was not available. Testing was conducted in the following order 1) vacuum exposure analysis and testing, 2) random vibration, 3) thermal cycling, and 4) radiation exposure. This testing and analysis is typically performed on optical fiber assemblies to assure their reliable performance in a space environment [1-4]. Prior to any testing the FLEX-LITE™ cable was thermally preconditioned to provide greater thermal stability with regards to induced shrinkage. Preconditioning involves 8 thermal cycles, with 60 minute soaks at +60ºC, 25 minutes at –20ºC and ramp rates of less than 2ºC/min.
Three of the FON1173 FLEX-LITE™ with Diamond AVIMs cable assemblies were tested for vibration and thermal, respectively, and optically monitored in-situ during the environmental exposure. For radiation exposure, 10 meters of each cable type FON1173 and FON1174 were tested under two different dose rate conditions while maintained at –20ºC. All optical performance testing was conducted at 850 nm.

2. EXPERIMENTAL

2.1 Materials Characterization

The W.L.Gore FLEX-LITE™ cable with acrylate coated fiber was tested, un-terminated, to the ASTM-E595 but in a full configuration and it was approved for space flight use with a TML < 0.35 %.[3]. The EpoTek 353ND epoxy is listed in the outgassing database and is approved for space flight use.[5] The Hytrel 8068 AVIMS connector boots must be preconditioned in a vacuum environment (between 10^2 torr & 1 torr) at 140ºC for 24 hours in order to pass the standard vacuum outgass test requirement of the ASTM-E595. Preconditioned or "degassed" boots were tested to ASTM-E595 and the results were: average TML of 0.48% and average CVCM of 0.10%. The test results indicate that the boots that have been "degassed" by the preconditioning procedure mentioned can be used in a space flight environment.

[*] melanie.ott@gsfc.nasa.gov, 301-286-0127, nepp.nasa.gov/photonics or misspiggy.gsfc.nasa.gov/photonics

2.2 Vibration Characterization

The following is the number designation of the three cable sets that were exposed to environmental conditions of vibration and temperature. Also included in Table 1 is the insertion loss and visual inspection measurements prior to any environmental testing. Each individual assembly listed in column two was approximately 24 inches long.

Table 1: Cable Assembly Designations and Mated Pair Assignments.

Cable Test Set	Cable Number Designation	Mated End of EP assembly	Insertion Loss @ 850 nm	Endface Side A	Endface Side B
MP1-1	EP-MLA-7	Side A	0.385 dB		
MP1-2	EP-MLA-8	Side B	0.479 dB	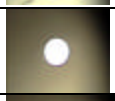	
MP2-1	EP-MLA-9	Side B	0.712 dB	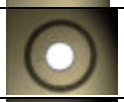	
MP2-2	EP-MLA-10	Side A	0.501 dB		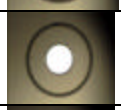
MP3-1	EP-MLA-11	Side B	0.285 dB		
MP3-2	EP-MLA-12	Side A	0.693 dB		

For vibration testing, the profile for random vibration was as follows:

Table 2: Random Vibration Profile for Testing of Assemblies

Frequency (Hz)	Protoflight Level
20	.026 g^2/Hz
20-50	+6 dB/octave
50-800	.16 g^2/Hz
800-2000	-6 dB/octave
2000	.026 g^2/Hz
Overall	14.1 grms

Each assembly, mated pair was tested for three minutes per axis, X, Y, and Z. Each mated pair was monitored actively or optically insitu as quickly as possible using the HP8153 optical power meter and a data acquisition Labview program. The instrument is capable of transmitting via GPIB no greater than 7 samples per second. An 850 nm optical LED source was used to transmit CW though the mated pair. The optical monitoring was started just prior to the vibration exposure and continued throughout the three-minute duration. The LED source was monitored throughout the testing as well such that source optical power fluctuations could be subtracted from the vibration induced optical power transients during data analysis. Figure 1, a and b, show images of the vibration fixturing with the assembly in the z axis orientation in (Figure 1a) and in the x axis orientation (Figure 1b). The fixturing alone was verified for random vibrations (to assure no resonance reactions within the specified vibration parameters) prior to attaching the optical assembly.

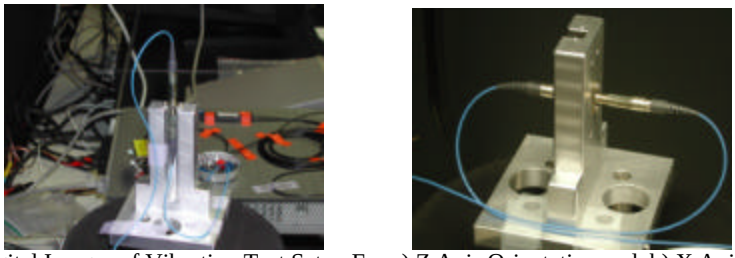

Figure 1: Digital Images of Vibration Test Setup For a) Z Axis Orientation and b) X Axis Orientation

Presented is the collected data for the mated pair assemblies during random vibration testing. To show an example of the data collected, Figures 2-3 are plots of the relative optical power for each axis orientation for MP1. Table 3, shown after the figures summarizes the information for all of the vibration tests conducted.

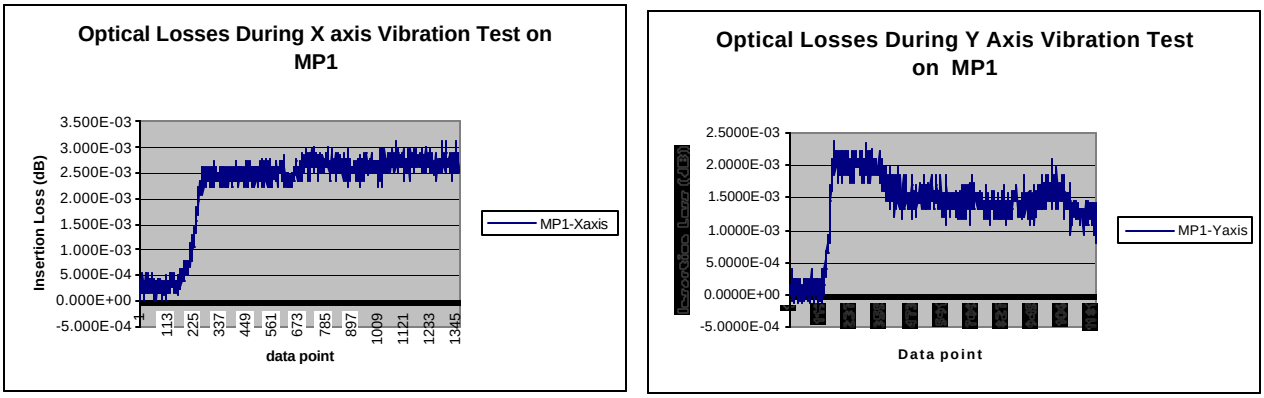

Figure 2: Optical Insitu Monitoring of the MP1 Assembly Set During 3 Minute Vibration Exposure along the a) X and b) Y axis.

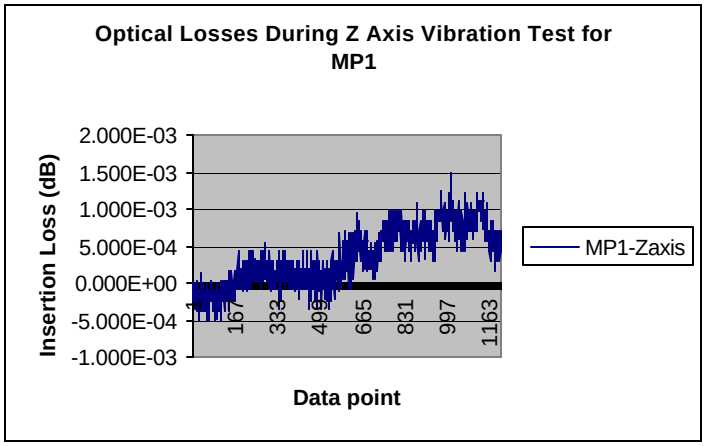

Figure 3: Optical Insitu Monitoring of the MP1 Assembly Set During 3 Minute Vibration Exposure along the Z axis.

Table 3: Summary of Vibration Performance Results

Assembly	Test Orientation	Max Vib Induced Insertion Loss	Overall Change, Insertion Loss, Post Vibration Testing	Comments on post vibration insertion loss
MP1	X axis	0.0031 dB	0.0028 dB	
MP1	Y axis	0.0024 dB	0.0012 dB	
MP1	Z axis	0.0015 dB	0.0006 dB	
MP2	X axis	0.0002 dB	-0.0027 dB	Power increase
MP2	Y axis	0.0006 dB	-0.0012 dB	Power increase
MP2	Z axis	0.0027 dB	0.0004 dB	
MP3	X axis	0.0005 dB	- 0.0017 dB	Power increase
MP3	Y axis	0.0004 dB	0.0000 dB	
MP3	Z axis	0.0003 dB	-0.002 dB	Power increase

As can be seen in the summary Table 3, most of the losses registered were negligible and many were very close to the detector noise floor. There were no vibration-induced losses that registered above 0.004 dB during testing and no final changes in performance greater than 0.003 dB. In several cases the power transmission increased by small amounts (less than .003 dB). A post vibration visual inspection was performed an all mated pairs and the resulting images showed no damage to any of the end faces.

2.3 Thermal Exposure Testing

Thermal cycling was conducted on the assemblies with the same mated pair (as specified in Table 1) that was connected to the fixturing during vibration testing. This mated pair was placed just inside of the thermal chamber. The three assemblies were tested simultaneously. The conditions were as such: –30ºC to +50ºC at a ramp rate of 2ºC/min for a total of not less than 30 cycles. The thermal extremes were maintained for 25 minutes each. The thermal chamber was monitored with a thermal couple to insure that a minimum of 32 cycles had indeed been conducted while the optical power was monitored. Due to data acquisition program failure the mated pair assemblies under test were cycled 48 cycles prior to any data being logged. Therefore, the data presented in Figure 4 is the data collected after the assemblies had been previously cycled 48 times. The number of cycles in Figure 4 totals 32 but the actual amount of cycles that occurred after the initial 48 cycles, totaled 42. Figures 5a and 5b show digital images of the experimental set up. Figure 5a shows the three mated assemblies inside of the thermal chamber and Figure 5b shows the equipment set up just outside of the thermal chamber.

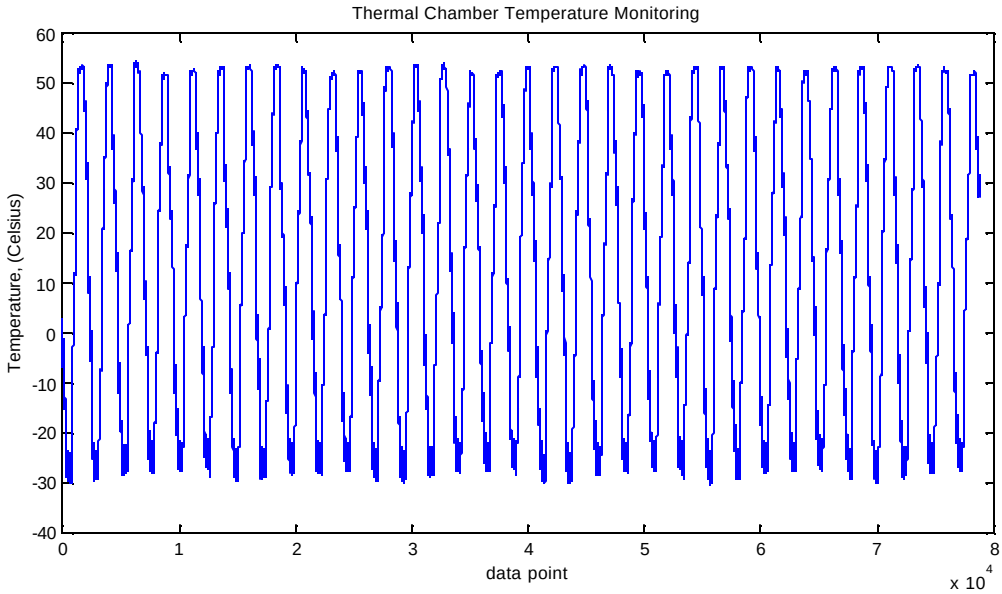

Figure 4: Thermal Chamber Temperature Measurements During Thermal Cycling (last 32 cycles of the 42 cycle session)

Figure 5a) Mated Pairs Inside of Thermal Chamber, 5b) Experimental Set up Used for Monitoring Optical Power During Testing

Figures 6 – 8 show the collected data for all three mated assemblies during the 42 thermal cycles of testing after the initial 48-cycle exposure. The data plots presented are the in-situ optical insertion loss measurements registered during exposure. Figure 9 is a plot of the insertion loss data from MP1 for relative cycle 20 through cycle 26 (absolute cycle 68 through 74) along with the collected data from the thermal couple that measured the temperature inside of the thermal chamber during testing. The point of showing a limited number of cycles is to view the pattern of the optical insertion loss along with changing temperature. The assemblies behave in a predictable manner, with the insertion loss increasing with decreasing temperature.

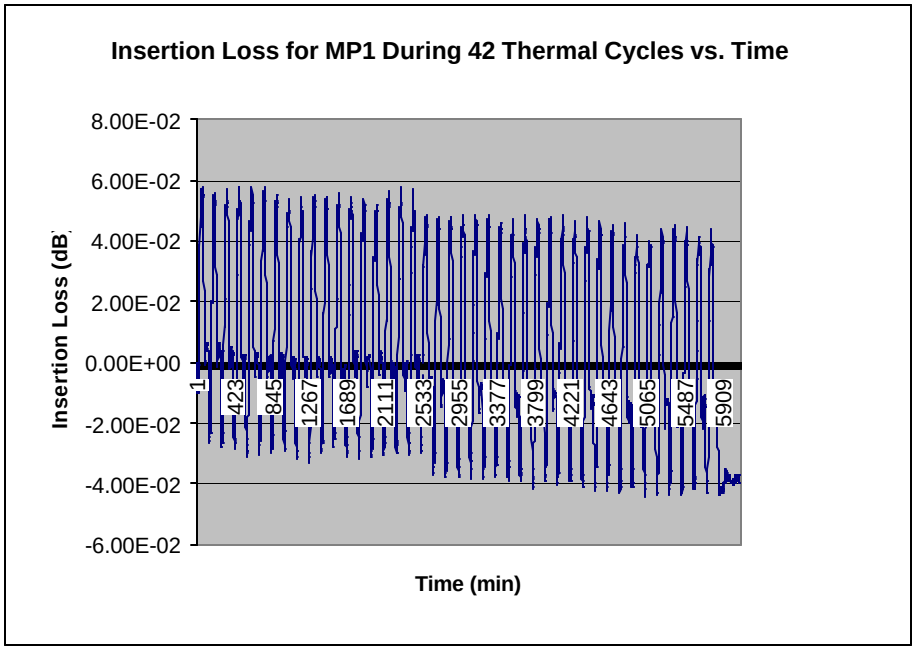

Figure 6: Insertion Loss Measurments During 42 Thermal Cycles for MP1.

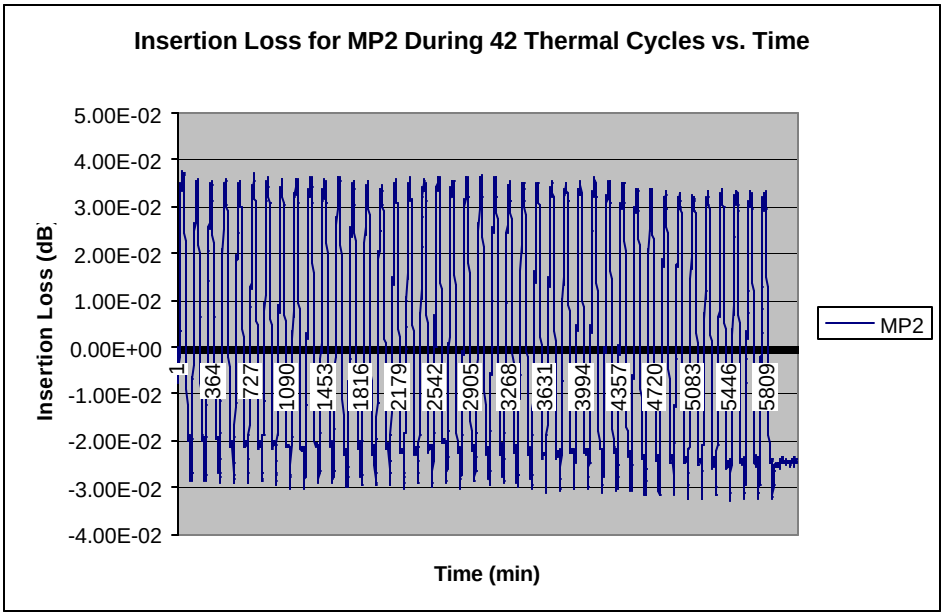

Figure 7: Insertion Loss Measurements During 42 Thermal Cycles for MP2.

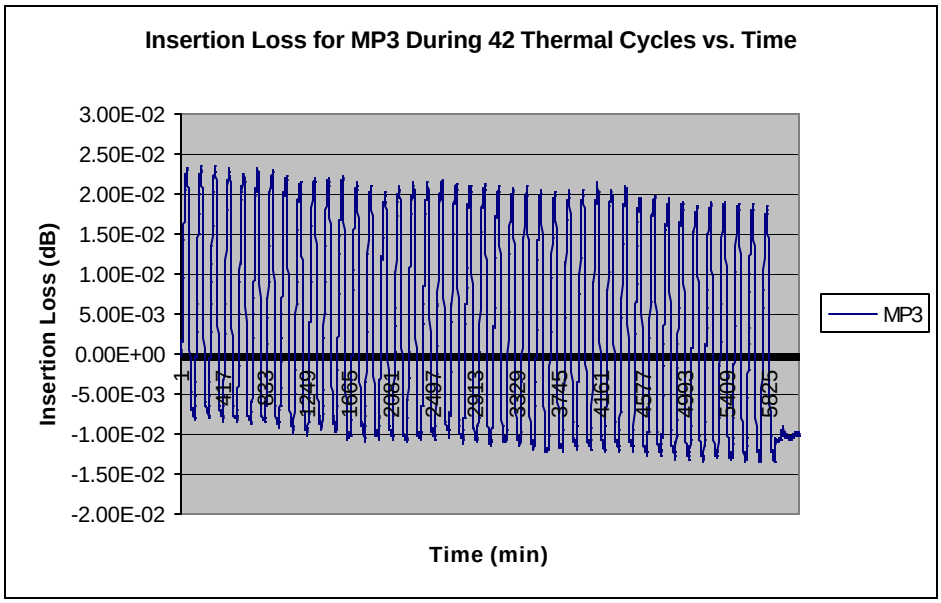

Figure 8. Insertion Loss Measurements During 42 Thermal Cycles for MP3**.**

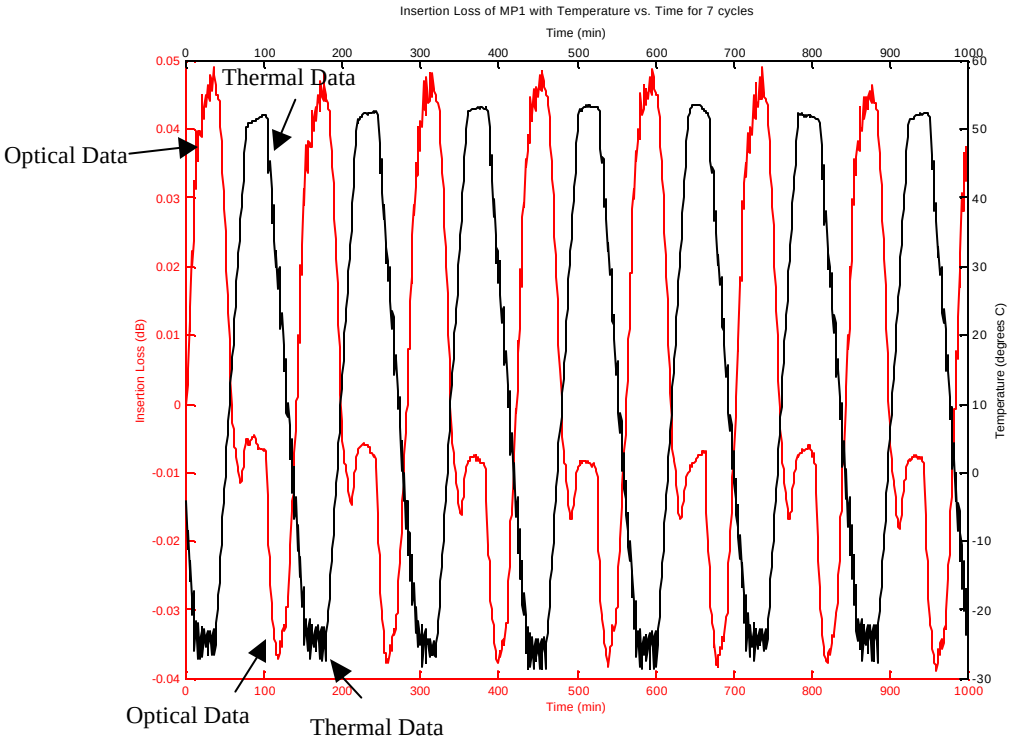

Figure 9: Insertion loss data of MP1 with thermal chamber data for cycle 20 through cycle 26

In all cases the assemblies showed an overall decrease in insertion loss (a negative number) or gain in optical power transmission as a result of thermal exposure to 90 thermal cycles. Below is a summary of the post thermal cycling measurements and visual inspections. Column one of Table 4 shows the difference between the maximum registered power and the minimum registered optical power for the entire test. In the second column of Table 4 the total change in

insertion loss is listed for each assembly. In the third column the insertion loss after the initial 48 cycles in which no in-situ data was recorded is listed for each assembly. The insertion loss after the additional 42 cycles in which in-situ data was recorded is listed in column four and in the fifth column, an overall insertion loss as compared to the power levels before any thermal cycling began is listed. The largest insertion loss registered during thermal cycling is listed in column six and the post thermal digital images of the mated pair that was in the thermal chamber are listed in the last two columns.

Table 4: Summary of Thermal Induced Effects on AVIMS Assemblies

Assembly	max Δ insertion loss during cycling	Post cycling insertion loss, first 48 cycles	Post cycling insertion loss, additional 42 cycles	Overall Change in insertion loss, 90 cycles.	Max Insertion Loss Registered during Testing	Post Thermal Visual Inspection MPX-1	Post Thermal Visual Inspection MPX-2
MP1	0.09 dB	-0.004 dB*	-0.04 dB	-0.044 dB	0.058 dB	Side A	Side B
MP1							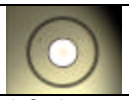
MP2	0.07 dB	0.015 dB	-0.03 dB	- 015 dB	0.037 dB	Side B	Side A
MP2							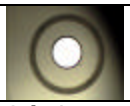
MP3	0.04 dB	-0.025 dB	-0.01 dB	-0.035 dB	0.024 dB	Side B	Side A
MP3							

*A negative insertion loss means a gain in optical power.

In summary, it can be seen by reading the information in Table 4 that the AVIMS assemblies performed quite well with no registered insertion losses during or after testing of more than .06 dB. In all cases the final output power was actually larger than prior to thermal exposure.

Comparing the results of the final insertion loss measurements from the vibration testing and the thermal testing it is clear that the effects from thermal testing dominate. However, if we choose the largest registered insertion loss measurement from all the axis orientation tests and add this loss to the final insertion loss after thermal testing the results are: MP1 power increase of ~0.04 dB, MP2 power increase of ~0.02 dB and MP3 power increase of ~0.04 dB. The performance of these assemblies has actually improved by a very slight amount after enduring 3 different vibration tests and 90 thermal cycles. The values of increase are not large enough to warrant concern and some of the increase can be associated with mating repeatability.

2.4 Total Dose Gamma Radiation Exposure Testing

The total ionizing radiation dose expected for MLA is 30 krads over an 8 year period. However, the assumption is that the solar active period will occur during the first 5 years. Using 5 years as the period of time during which the exposure to 30 krads will occur, the average dose rate will be 16.44 rads/day, .685 rads/hour, .011 rads/min. During the exposure, the worst case scenario for these assemblies in terms of thermal environments will require that they endure a cold temperature of -20ºC for a period of 5 years time without source power applied.

In order to extrapolate the high dose rate performance of the FLEX-LITE™ optical fiber cable to a low dose rate space environment, the two dose rate model was used that is typically used for multimode fiber. This model was developed by Friebele et al. for extrapolating high dose rate test data to actual low dose rate space environments.[6] The assumption for this model is that the optical fiber will attenuate faster at higher dose rates and so two tests are necessary for an extrapolation calculation to be attained through data analysis and comparison between the two different tests.

In the case of making technical assessments of optical fiber performance the worst case scenario is used; in other words, the coldest temperature and under dark conditions (no light propagation). Typically optical fiber will experience more radiation induced attenuation when not transmitting light and while kept in a cold environment thus inhibiting the thermal annealing properties of the fiber.[2,7-9] Therefore the parameters for this radiation test were based on both the two dose rate model while using the worst environmental conditions for radiation induced attenuation. The test was conducted at 850 nm, which again provided a more unfavorable scenario than using the actual MLA wavelength of 1064 nm. Many types of multimode optical fiber are more susceptible to radiation induced attenuation at lower wavelengths. [10]

Two tests were conducted on both the 200 micron core fiber FLEX-LITE™ FON1173 and the 300 micron core fiber FLEX-LITE™ FON1174 cable. Each cable was tested in 10 meter lengths at 22.7 rads/min for the high dose rate test and at 11.2 rads/min for the low dose rate test while kept at –20ºC. Exposure was conducted until a total dose of 30 krads was attained. The 850 nm power levels were maintained below 1 microwatt to simulate "dark" conditions and to avoid any photobleaching effects.

In Figure 10 the radiation induced attenuation for both fiber cables at the higher dose rate of 22.7 rads/min with the temperature maintained at –20ºC during exposure is shown up to the total dose of 30 krads. Figure 11 presents the data for both optical fiber cables under the same conditions but at the lower dose rate of 11.2 rads/min. Table 5 summarizes the conditions of the test including the data shown in Figures 12 and 13 that are graphs from monitoring of the thermal chamber. The last column in Table 5, lists the expected attenuation for the actual MLA assemblies of 26.1 inches (.663 m) based on the results of this testing.

Table 5: Summary of Radiation Induced Attentuation on MLA Assemblies

Part Number	**Fiber Type (microns)**	**Dose Rate**	**Atten @ 30 krads**	**Ave.Temp during Test**	**Expected Atten 26.1 inches @ 30 krads**
FON1173	200	11.2 rads/min	1.024 dB	-24.1 ºC	.068 dB
FON1174	300	11.2 rads/min	0.917 dB	-24.1 ºC	.061 dB
FON1173	200	22.7 rads/min	0.892 dB	-18.3 ºC	.059 dB
FON1174	300	22.7 rads/min	0.818 dB	-18.3 ºC	.054 dB

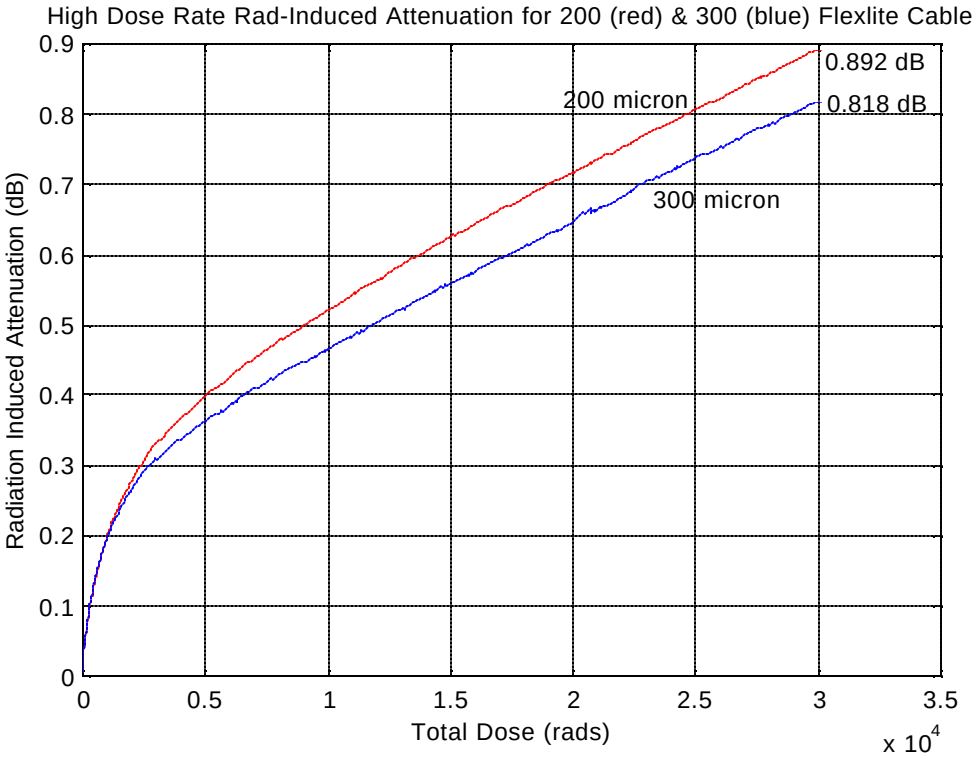

Figure 10: High Dose Rate Test Results to 30 krads of the 200 and 300 micron Optical Fiber FLEX-LITE™ Cable (10 meters).

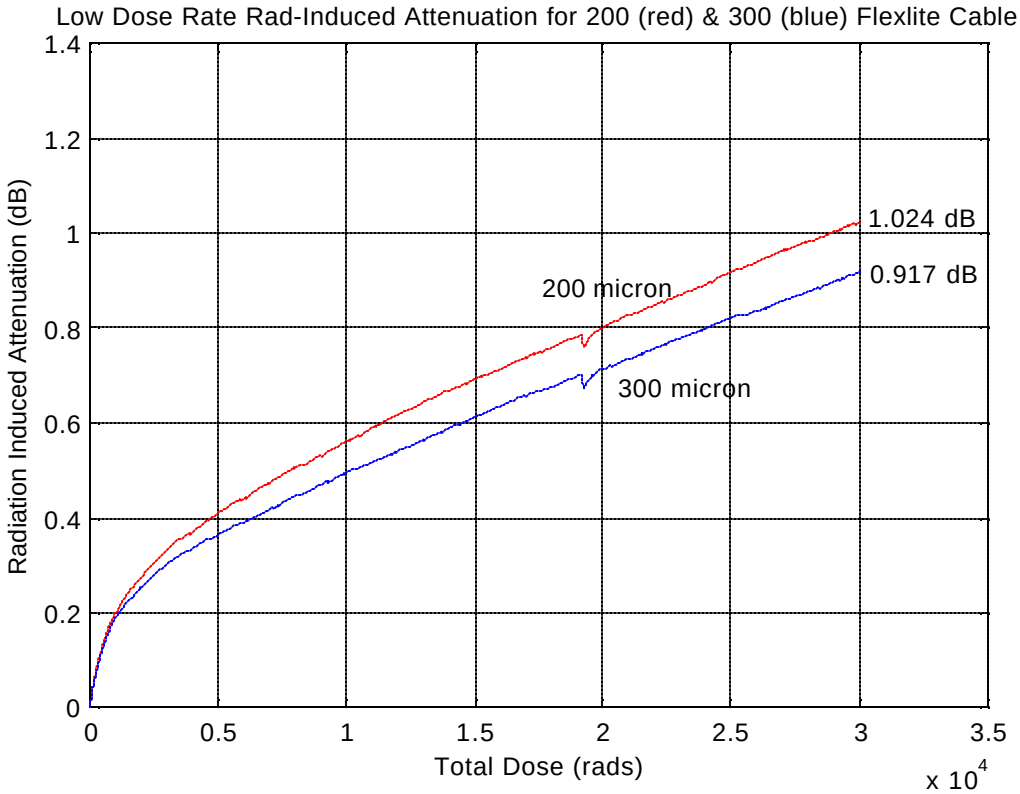

Figure 11: Low Dose Rate Test Results to 30 krads of the 200 and 300 micron Optical Fiber FLEX-LITE™ Cable (10 meters).

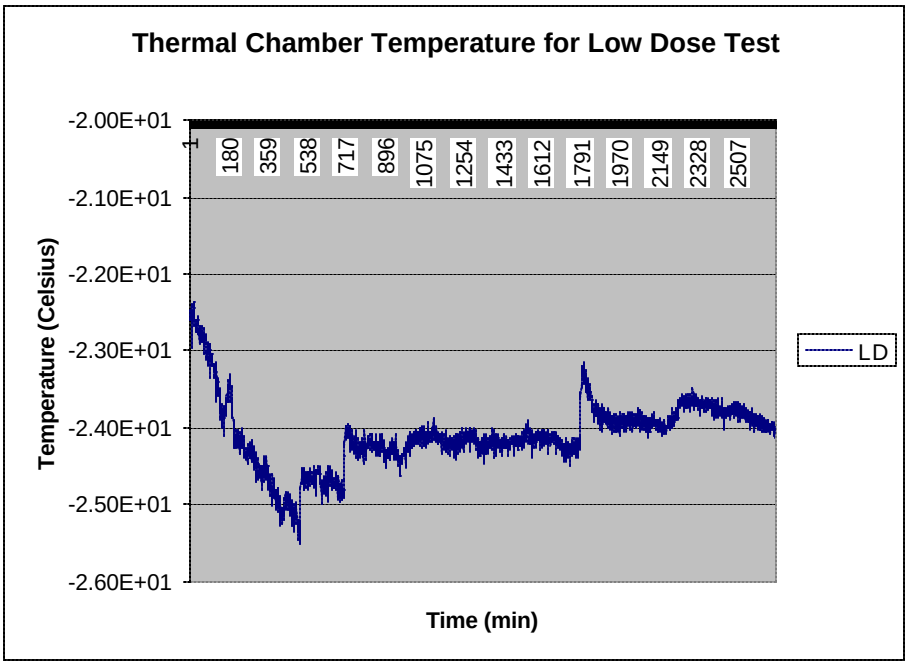

Figure 12: Thermal Chamber Temperature Monitoring During the Low Dose Rate Test.

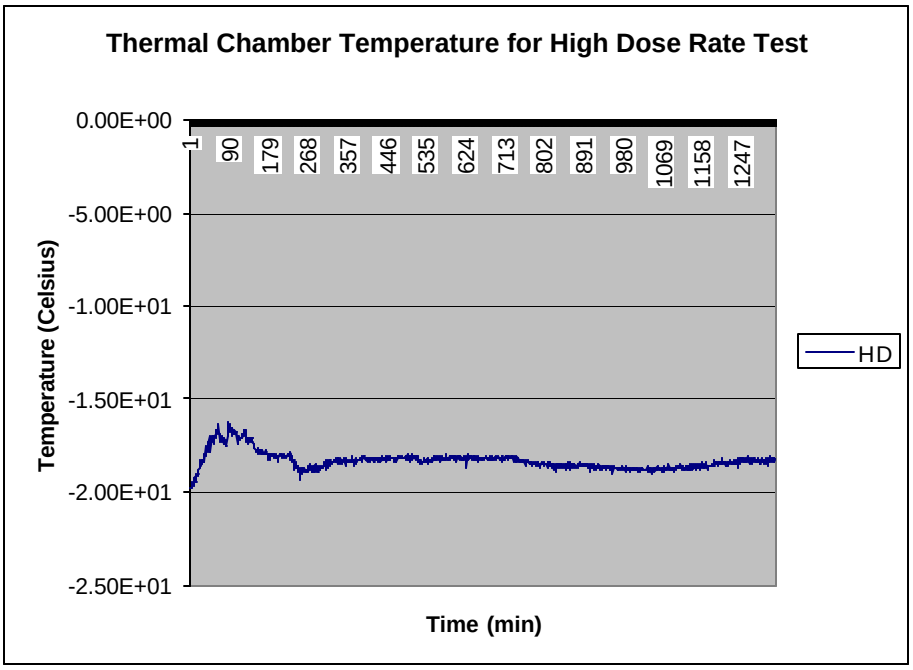

Figure 13: Thermal Chamber Temperature Monitoring During the High Dose Rate Test.

In Figure 11 the slight "glitch" seen at approximately 20 krads was due to the activated fire alarms in the building that houses the cobalt 60 chamber. For safety reasons the shutter on the cobalt 60 chamber was closed for approximately 7 minutes during the time that the fire alarms were activated. The impact on the outcome of those results is negligible due to the overall data analysis discussed in more details below.

In Table 5 it is evident that the performance of the assemblies under different dose conditions is nearly identical. In most cases, when the dose rate is changed by a factor of two there is usually a discernable difference that allows usage of the two dose rate model for extrapolation purposes. It may be that the data would fit the model if the second dose rate test were a test that is an order of magnitude higher and in this case an extrapolation would be possible but such data is not available at this time. Therefore, in this case, there is very little difference in the performance and the model can not be used to extrapolate to a much lower dose rate. Testing at the actual dose rate would take as long as the mission so it is not a feasible method for determining the radiation induced attenuation. The only conclusion that can be made by the results of this testing is that the radiation induced attenuation expected during the 5 years will not exceed .07 dB (or drop below 98.4% transmission) for each of the MLA assemblies when the total dose reaches 30 krads while exposure to dark conditions and a temperature of –20ºC. This conclusion is of course made given the worst possible conditions of the environmental parameters as stated previously.

The higher radiation induced attenuation that was registered during the lower dose rate testing was most likely due to the fact that the thermal chamber was running colder than the temperatures that were registered during the higher dose rate testing. This can be seen in summary Table 5. The difference in radiation induced attenuation between the high dose rate test and the low dose rate test is small enough to be considered the same since there was a difference in the thermal environments.

3. CONCLUSIONS

Presented here is the data and analysis of the environmental testing of the FLEX-LITE™ assemblies with Diamond AVIMS connectors. Materials were analyzed for performance in a vacuum environment, and the assemblies were tested for losses induced by thermal, random vibration and radiation exposure. As compared to assemblies that have been tested in the past by other programs these assemblies performed with superiority. [1-3]

ACKNOWLEDGMENTS

The authors would like to thank the MESSENGER, Mercury Laser Altimeter program and the NASA Parts and Packaging Program for funding this work, Dr. Henning Leidecker for always lending enthusiastic support, and Darryl

Lakins Office Chief of Code 562 for resources support, Luis A Ramos-Izquierdo (MLA), Arlin Bartels (MLA), Phillip Zulueta (EPAR NEPP), and Dr. Charles Barnes (NEPP) for programmatic support.

REFERENCES

1. Melanie N. Ott, Jeannette Plante, Jack Shaw, M. Ann Garrison-Darrin, "Fiber Optic Cable Assemblies for Space Flight Applications: *Issues and Remedies,"* Paper 975592 SAE/AIAA 1997 World Aviation Congress, October 13-16, Anaheim, CA.
2. Melanie N. Ott, "Fiber Optic Cable Assemblies for Space Flight II: Thermal and Radiation Effects," Photonics For Space Environments VI, Proceedings of SPIE Vol. 3440, 1998, pages 37-46.
3. Melanie N. Ott, Patricia Friedberg, "Technology validation of optical fiber cables for space flight environments," Optical Devices for Fiber Communication II, Proceedings of SPIE Vol. 4216, 2001, pages206-217.
4. Melanie Ott, "*Assurance of COTS Fiber Optics Cable Assemblies for Space Flight*," Presentation to the Electronic Components for the Commercialization of Military and Space Systems Conference, Los Angeles CA, February 10, 1999.
5. Outgassing Data for Selecting Spacecraft Materials Online, URL is http://epims.gsfc.nasa.gov/og/
6. E. J. Friebele, M.E. Gingerich, D. L. Griscom, "Extrapolating Radiation-Induced Loss Measurements in Optical Fibers from the Laboratory to Real World Environments", 4th Biennial Department of Defense Fiber Optics and Photonics Conference, March 22-24, 1994.
7. Melanie Ott, "TID Radiation Induced Attenuation Testing at 1300 nm Using ISS Requirements on Three Optical Fibers Manufactured by Lucent SFT," September 2000, Report to Lucent and NASA publication for Web.
8. Ken LaBel, Cheryl Marshall, Paul Marshall, Philip Luers, Robert Reed, Melanie Ott, Christina Seidleck and Dennis Andrucyk, "*On the Suitability of Fiber Optic Data Links in the Space Radiation Environment: A Historical and Scaling Technology Perspective,"* IEEE Aerospace Conference, Vol. 4, pp. 421-434.
9. Melanie Ott, "*Radiation Effects on Commercially Available Optical Fiber*," IEEE Nuclear Science and Radiation Effects Conference, Proceedings of the IEEE Nuclear and Space Radiation Effects Conference Data Workshop 2002, pages 24-31.
10. Melanie Ott, "*Radiation Hardness of Optical Fiber*," Tutorial presentation to the Space Parts Working Group, Sept, 1997, presentation can be found at the website URL: http://misspiggy.gsfc.nasa.gov/photonics/ under the subject of "Radiation Effects".
11. Diamond Part numbers for connectors are D-6206.1 with custom drilled ferrules part number E070040095VNAS1 (200 core fiber), E070040095VNAS2 (300 micron core fiber), boot part number 070015048V001. Polymicro Technologies part numbers for fiber are: FIA200220500 (200 micron core fiber), and FIA300330500 (300 micron core fiber).
12. For more information please see the website nepp.nasa.gov/photonics